

Original

Shen, J.; Suhuddin, U.F.H.; Barbosa, M.E.B.; dos Santos, J.F.:

Eutectic structures in friction spot welding joint of aluminum alloy to copper

In: Applied Physics Letters (2014) AIP

DOI: 10.1063/1.4876238

Eutectic structures in friction spot welding joint of aluminum alloy to copper

Junjun Shen,^{a)} Uceu F. H. Suhuddin, Maria E. B. Cardillo, and Jorge F. dos Santos

Helmholtz-Zentrum Geesthacht, Institute of Materials Research, Materials Mechanics, Solid-State Joining Processes, Max-Planck-Str. 1, 21502 Geesthacht, Germany

(Received 3 April 2014; accepted 27 April 2014; published online 12 May 2014)

A dissimilar joint of AA5083 Al alloy and copper was produced by friction spot welding. The Al-MgCuAl₂ eutectic in both coupled and divorced manners were found in the weld. At a relatively high temperature, mass transport of Cu due to plastic deformation, material flow, and atomic diffusion, combined with the alloy system of AA5083 are responsible for the ternary eutectic melting. © 2014 AIP Publishing LLC. [<http://dx.doi.org/10.1063/1.4876238>]

Al/Cu combination joint has been widely applied in industries for its mass and cost reduction.¹ One key factor to constrain its application is the joining technique. Traditional fusion welding methods are rarely used due to differences in materials properties and the formation of brittle intermetallic compounds.²⁻⁴

Friction spot welding (FSpW), also known as refill friction stir spot welding, is able to join two or more materials in a spot-like lap joint configuration.⁵ The principle of FSpW has been present elsewhere.⁶ Because of its solid-state character and advantages, such as good mechanical properties and keyhole-free surface, FSpW has been used for joining similar materials and dissimilar materials, for instance, aluminum and magnesium alloys^{6,7} (hereafter referred to as Al/Mg). However, in dissimilar FSpW, eutectic melting or constitutional liquation has been observed. For example, Suhuddin *et al.*⁶ reported formation of eutectic structures in dissimilar Al/Mg welds produced by FSpW. Similar eutectic melting was also found in dissimilar joints produced by other friction-based welding methods.⁸⁻¹⁰ In all these cases, eutectic systems were binary, the components either from two base metals^{6,8,9} or from one base metal and the coating.¹⁰ The reason for eutectic melting is believed to be attributed to high temperature exposure (close to the solidus temperature) and enhanced mutual diffusion resulted from plastic deformation. Compared with solid, the presence of liquid will significantly accelerate atomic diffusion and consequently increase the formation possibility of intermetallic, which is always undesirable due to a negative influence on mechanical properties of dissimilar joints. Also the presence of liquid could cause problems associated with fusion welding, such as elemental segregation and solidification cracking. Therefore, it is particularly critical for understanding the origin of eutectic melting during FSpW of dissimilar materials. Up to now, the dissimilar FSpW of aluminum alloys and copper (hereafter referred to as Al/Cu) has not been reported yet. The present research investigates the eutectic structures in friction spot welded dissimilar materials, AA5083 aluminum alloy and copper, by combined energy dispersive X-ray (EDS) and electron backscatter diffraction (EBSD) technique, and discusses the microstructural evolution during dissimilar FSpW.

Commercially available AA5083 Al alloy and phosphorus deoxidized copper sheets (100 × 25 × 2 mm³) were welded by an RPS 100 friction spot welding machine using the sleeve-plunge variant. The main process parameters were rotation rate, 2000 rpm, sleeve plunge depth, 2 mm, and dwell time, 1 s. In order to reduce heat input, the AA5083 Al alloy was placed at the top of copper.

Prior to metallographic analysis, the joint was sectioned around the weld centerline, ground and polished, and then etched by Keller reagent. The macrostructure features were examined by an optical microscope (OM). Followed by polishing on a cross section polisher, the specimen was analyzed by a scanning electron microscope (SEM) equipped with an EDS analysis system. Additionally, the TSL Delphi package, a system integrated EDS and an EBSD system were used to identify the phases by indexing the Kikuchi patterns based on elemental composition. The powder diffraction file database, ICDD PDF-4+, was used for phase retrieval and identification. To improve the reliability, only grains with a confidence index (CI) higher than 0.1 and angle fit less than 1° were used for the phase identifications.

Figure 1(a) shows a typical macrostructure of Al/Cu dissimilar FSpW joint overlaid with the tool profile (dashed white lines). The weld nugget is symmetrically drum-shaped. Its size is obviously larger than the outer diameter of the sleeve. This effect may be associated with the tool design and the material flow. For the same reason, a cave was formed on the Al/Cu interface right beneath the sleeve end face. The rim of the weld nugget shows a completely different contrast. It might be caused by a special thermo-mechanically process, which will be investigated in a future work.

Close to the Al/Cu interface, location indicated by the yellow box in Fig. 1(a) and shown in Fig. 1(b), several microconstituents with characteristics of eutectic structure are formed. More details are shown in Fig. 1(c). There are four distinct microconstituents, marked by A, B, C, and D. A, the dark matrix, is the pre-eutectic phase. B, consisting of alternating layers (dark and bright lamellae), namely, two-phase structure, is the coupled eutectic. C, the bright isolated island-like lamellae, distributed along the grain boundary of the pre-eutectic phase, is the divorced eutectic. D forms a rounded equilateral triangle shape and seems to be independent of the eutectic system.

According to the EDS maps of selected area from the eutectic region (indicated by dashed white box in Fig. 1(b)),

^{a)} Author to whom correspondence should be addressed. Electronic mail: junjun.shen@hzg.de

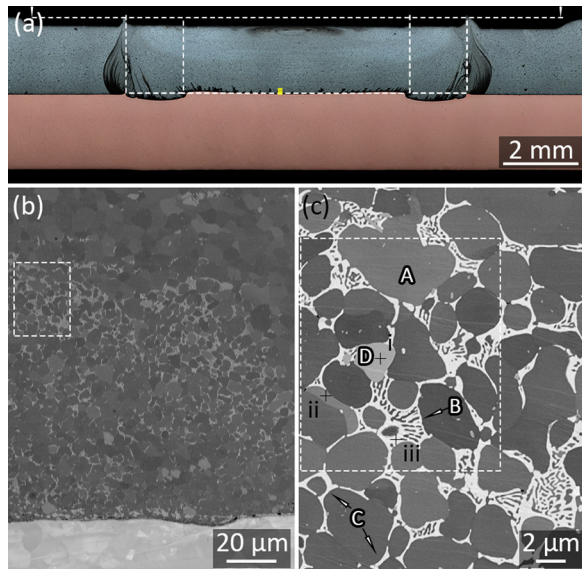


FIG. 1. (a) Macrostructure of the weld cross-section (optical image after etching by Keller etchant, dashed white lines show the tool profile overlaying on the weld); (b) the partial-dissolved Al/Cu interface and the region with features of eutectic structure, taken from the location marked with yellow box in (a); (c) detail of the eutectic region, taken from the white box in (b).

the matrix A contains dominant Al as well as a small amount of Cu and Mg, and thus it is the primary α -Al, shown in Fig. 2; divorced eutectic C significantly consists of Al, Cu, and Mg; the dark phase in coupled eutectic B is mainly rich in Al and hence it is the eutectic α -Al, while the bright one resembles eutectic C; D is also Al-rich but depleted in Cu or Mg. To identify these phases here, however, direct quantitative EDS analysis is unreliable, since the dimension of the eutectic structures is typically submicron (see Fig. 2(c)) and thus beyond the spatial resolution of EDS in SEM. Therefore, the

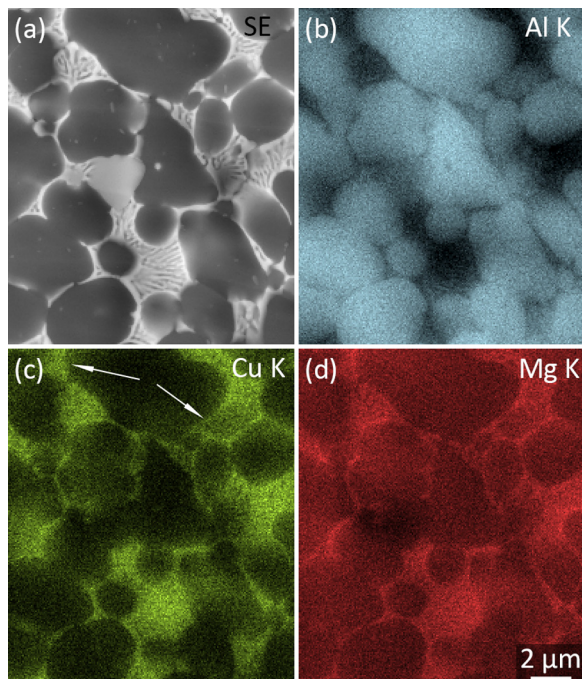


FIG. 2. EDS maps show the distribution of each element (a) field of view, (b) Al, (c) Cu, and (d) Mg (taken from the location marked with dashed white box in Fig. 1(c)).

EBSD technique, due to its diffraction-based origins and higher lateral spatial resolution, supplemented with EDS, is adopted to determine the structural and elemental component.

Results of the phase identification of the eutectic structures are partially (only points i, ii, and iii marked in Fig. 1(c)) shown in Fig. 3. Several results can be obtained. First, phase D, e.g., point i, can be indexed as $\text{Al}_6(\text{Mn}, \text{Fe})$, which is considered as a common dispersoid in Al 5xxx alloys (Al-Mg-Mn alloy) shown as large particles after solidification.¹¹ Second, the lattice parameters of primary α -Al (point ii) are hardly influenced by the minor Cu and Mg contents, indicating the concentrations of Cu and Mg are still within the solid solubility. Third, the other eutectic phase in the coupled eutectic structure in addition to eutectic α -Al or the divorced eutectic can be confidently indexed as MgCuAl_2 (designated by the symbol S). Its formation mechanism will be discussed later.

Nevertheless, composition variations of Cu in the primary α -Al grains could be clearly revealed by the EDS maps (see Fig. 2). That is so-called microsegregation. The reason for segregation is the rapid cooling or non-equilibrium cooling condition, imposed by the FSpW process. Upon cooling, the Cu component is expelled from the grain interior of supersaturated Al to the grain boundary. However, the further diffusion of Cu has been frozen before completion by the drastically reduced temperature. Therefore, a diffusive feature could be seen, e.g., from the matrix center to the eutectic, the concentration of Cu increases, shown by two arrows in Fig. 2.

It should be noted that the base metal AA5083 is nearly free of Cu. Hence, the only possibility is that the copper sheet supplies as the source of Cu for the eutectic region. However, as shown in Fig. 1(b), the distance between the eutectic region and the original Al/Cu interface is about

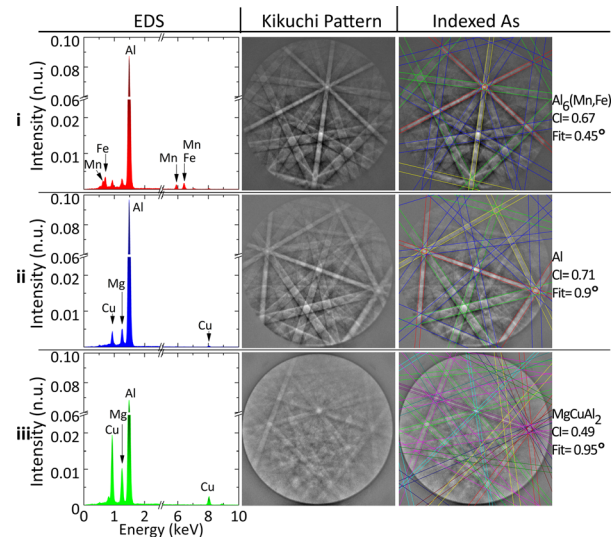


FIG. 3. EDS spectra and the corresponding Kikuchi patterns of points i, ii, and iii on Fig. 1(c), obtained by TSL Delphi package, show the phase identification process by integrated EDS and EBSD. The intensity is normalized with respect to the sum (the total intensity measured from the full scale). That is, the total area of the region under the curve is 1. It should be noted that the identification of $\text{Al}_6(\text{Mn}, \text{Fe})$ was based on the data file of Al_6Fe , which possesses the same crystal structure and similar lattice parameters with Al_6Mn .^{11,12}

0.1 mm. It is probably impractical only by means of atomic diffusion to transfer Cu over such a long distance within the dwell time. A recent work on dissimilar friction stir spot welding of AA6061 to Cu¹³ shows that Cu-based fragments are observed in the upper part of the weld. This indicates that the initial mass transport of Cu, in the form of fragments, is due to the material flow (resulted from tool friction and rotation) as well as the intensive plastic deformation. It is noteworthy no isolated Cu or Cu-based fragments could be found in the present work. This is probably attributed to the fact that the sleeve did not penetrate into the Cu sheet. The subsequent mass transport is due to diffusion in solids. Under static conditions, diffusion is a thermal-activated physical process. While under non-equilibrium conditions, in addition to thermal-activated, it is also deformation-dependent. On one hand, the relatively high heat generated by the process enhances the atomic diffusion. On the other hand, a severe plastic deformation process as observed in friction-based welding will produce substantial crystal defects, such as vacancies and dislocations. These defects are believed to facilitate short-circuit diffusion (including pipe diffusion and grain boundary diffusion) and hence significantly increase the diffusion rate.¹⁴

In summary, the eutectic structures present in the Al/Cu weld are mainly α -Al-S eutectic in both the coupled and divorced manners. The reason for the eutectic melting can be interpreted as mass transport resulted from plastic deformation, material flow, and atomic diffusion as well as the relatively high temperature exposure. During penetration of the sleeve, the materials (Al base metal) will be forced into the cylinder chamber left by the pin. When the sleeve end approaches the Al/Cu original interface, because of the sleeve motion and material plastic deformation, a part of Cu will be detached off and transported into upper region of the weld. These isolated Cu fragments will be consumed by diffusing into the surrounding Al matrix. Then, in some localized regions, a certain eutectic system could be formed. Once the temperature reaches the eutectic point, constitutional liquation will take place. Liquation also accelerates the atomic diffusion and becomes more extensive. Upon rapid cooling, eutectic structures form in the joint. Meanwhile, some eutectic α -Al grains grow into the matrix indistinguishable from the primary α -Al leaving only the eutectic S visible, i.e., divorce eutectic.

The formation of S phase has not been previously mentioned in dissimilar friction-based welding of Al/Cu, mainly 6xxx^{2,13} or 1xxx Al alloy¹⁵ and copper. Therefore, the special alloy system of base metal AA5083 also contributes to the eutectic liquation. The welding thermal cycling measured by thermocouple indicates that the maximum peak temperature is 492 °C, which is obviously lower than either the Al-Cu binary eutectic point (about 548 °C¹⁶) or the AA5083 solidus temperature (about 590 °C¹⁷). This implies that the eutectic liquation cannot occur in the form of binary if the welding conditions hardly influence these eutectic and solidus temperatures.

According to Ref. 18, around the Al-rich corner of the Al-Cu-Mg ternary system, at the temperature close to 492 °C, there are two possibilities of eutectic reaction. At around 503 °C, one ternary eutectic occurs in the form of

Liquid $\rightleftharpoons \theta + (\text{Al}) + \text{S}$ (The symbol θ designates CuAl_2) and at around 508 °C another ternary eutectic occurs in the form of Liquid $\rightleftharpoons (\text{Al}) + \text{S}$. In this study, the presence of θ either close to the α -Al-S eutectic structure or the divorced S eutectic was seldom observed. As mentioned earlier, on the EDS map (see Fig. 3), the areas rich in Cu are also rich in Mg. Or, in addition to α -Al, only the phase rich in both Cu and Mg can be observed in the eutectic structures. Accordingly, the eutectic melting in Al/Cu joint is in the form of Liquid $\rightleftharpoons (\text{Al}) + \text{S}$.

It is worthy to note that the eutectic point of Liquid $\rightleftharpoons (\text{Al}) + \text{S}$ is higher than the measured maximum peak temperature in the weld. This indicates that the eutectic point is lowered under the intensive plastic deformation when compared to the equilibrium conditions. Also it is of interest that the eutectic reaction with higher eutectic point occurred instead of the one with lower eutectic point. This can probably be explained by the calculated isothermal section of ternary Al-Cu-Mg system (adapted from Ref. 18), shown in Fig. 4. Considering the quantitative result of the EDS maps around this eutectic region, the average atomic concentrations of Al, Cu, and Mg are about 90%, 4%, and 6%, respectively; the composition point falls into two-phase zone, (Al) + S, as shown by the red star in Fig. 4. Accordingly, it is reasonable that only the eutectic structures free of θ are present in the weld. Moreover, this composition point is much closer to the (Al) than the eutectic composition (73.5Al-12.6Cu-13.9Mg,¹⁸ the position not shown here). According to the Lever Rule, much more primary α -Al will be formed during cooling until the eutectic composition is achieved. As shown in Fig. 4, the dashed red line (its extension line passes through the vertex of pure Cu component in the composition triangle) corresponds to the alloy with a constant atomic ratio of 94Al-6Mg, which is approximately identical to the elemental ratio of Al to Mg in the AA5083 base metal. Assuming that there is no segregation of Mg solute in the α -Al matrix, upon further cooling, in addition to (Al) + S eutectic, Cu precipitates from (Al) with its concentration following along this line to the solid solubility. The precipitation of Cu is, however, incomplete due to rapid cooling, which results in segregation in (Al).

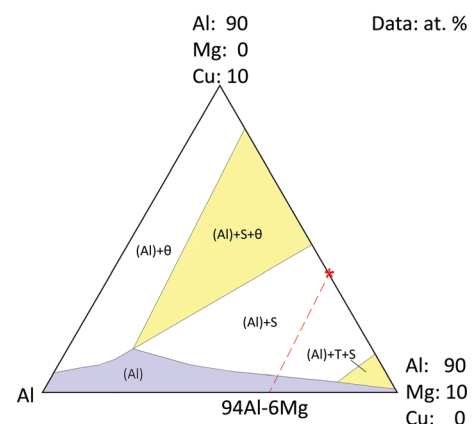


FIG. 4. Isothermal section of ternary Al-Cu-Mg phase diagram at 400 °C, $\theta = \text{CuAl}_2$, $\text{S} = \text{MgCuAl}_2$, and $\text{T} = (\text{Cu}_{1-x}\text{Al}_x)_{49}\text{Mg}_{32}$ (adapted from Ref. 18). Along the dashed red line the atomic fraction is a constant, 94Al-6Mg. And at the red star, the composition point is 90Al-4Cu-6Mg, namely, the average composition of the eutectic region, shown with the dashed white box in Fig. 2(c).

Eutectic structures are usually undesirable for the weld because of high cracking tendency. In the present research, however, there is no evidence of crack formation within the weld. This could be related to the local mechanical properties of the eutectic structures, which need to be further investigated.

Eutectic liquation in the Al/Cu dissimilar FSpW joint has been investigated. The main eutectic production includes Al-MgCuAl₂ eutectic structures and divorced MgCuAl₂ eutectic structures. In addition to mass transport by material flow and atomic diffusion at elevated temperature under the condition of severe plastic deformation, the alloy system of AA5083 also accounts for the ternary eutectic melting.

The authors are grateful to Dr. Zhiwu Xu and Dr. Junjie Zhang from Harbin Institute of Technology for helpful discussions.

- ¹J. P. Bergmann, F. Petzoldt, R. Schuerer, and S. Schneider, *Weld. World* **57**, 541–550 (2013).
- ²J. H. Ouyang, E. Yarrapareddy, and R. Kovacevic, *J. Mater. Process. Technol.* **172**, 110–122 (2006).
- ³H. J. Liu, J. J. Shen, L. Zhou, Y. Q. Zhao, C. Liu, and L. Y. Kuang, *Sci. Technol. Weld. Joining* **16**, 92–99 (2011).
- ⁴T. A. Mai and A. C. Spowage, *Mater. Sci. Eng. A* **374**, 224–233 (2004).
- ⁵C. Schilling and J. F. dos Santos, “Method and device for linking at least two adjoining work pieces by friction welding,” European patent EP 1230062 B1 (WO 2001/036144) (May 17, 2006).
- ⁶U. F. H. Suhuddin, V. Fischer, and J. F. dos Santos, *Scr. Mater.* **68**, 87–90 (2013).
- ⁷U. Suhuddin, V. Fischer, F. Kroeff, and J. F. dos Santos, *Mater. Sci. Eng. A* **590**, 384–389 (2014).
- ⁸Y. S. Sato, S. H. C. Park, M. Michiuchi, and H. Kokawa, *Scr. Mater.* **50**, 1233–1236 (2004).
- ⁹A. Gerlich, P. Su, and T. H. North, *Sci. Technol. Weld. Joining* **10**, 647–652 (2005).
- ¹⁰T. Liyanage, J. Kilbourne, A. P. Gerlich, and T. H. North, *Sci. Technol. Weld. Joining* **14**, 500–508 (2009).
- ¹¹Y. J. Li, W. Z. Zhang, and K. Marthinsen, *Acta Mater.* **60**, 5963–5974 (2012).
- ¹²L. Walford, *Acta Crystallogr.* **18**, 287–291 (1965).
- ¹³R. Heideman, C. Johnson, and S. Kou, *Sci. Technol. Weld. Joining* **15**, 597–604 (2010).
- ¹⁴J. Poirier, *Creep of Crystals: High-Temperature Deformation Processes in Metals, Ceramics, and Minerals* (Cambridge University Press, New York, 1985).
- ¹⁵P. Xue, D. R. Ni, D. Wang, B. L. Xiao, and Z. Y. Ma, *Mater. Sci. Eng. A* **528**, 4683–4689 (2011).
- ¹⁶J. L. Murray, *Int. Met. Rev.* **30**, 211–234 (1985).
- ¹⁷J. R. Davis, *Properties and Selection: Nonferrous Alloys and Special-Purpose Materials*, 10 ed. (ASM International, 1990).
- ¹⁸G. Effenberg and A. Prince, updated by N. Lebrun, H. L. Lukas, and M. G. Harmelin, “Al-Cu-Mg (Aluminium–Copper–Magnesium),” *Light Metal Systems, Part 2*, edited by G. Effenberg and S. Ilyenko (Springer Berlin Heidelberg, 2005).